Clim Dyn
DOI 10.1007/s00382-011-1195-x

Observed and simulated impacts of the summer NAO in Europe: implications for projected drying in the Mediterranean region

Ileana Bladé · Brant Liebmann · Didac Fortuny · Geert Jan van Oldenborgh

Received: 6 April 2011 / Accepted: 14 August 2011

Abstract Climate models predict substantial summer precipitation reductions in Europe and the Mediterranean region in the twenty-first century, but the extent to which these models correctly represent the mechanisms of summertime precipitation in this region is uncertain. Here an analysis is conducted to compare the observed and simulated impacts of the dominant large-scale driver of summer rainfall variability in Europe and the Mediterranean, the summer North Atlantic Oscillation (SNAO). The SNAO is defined as the leading mode of July–August sea level pressure variability in the North Atlantic sector. Although the SNAO is weaker and confined to northern latitudes compared to its winter counterpart, with a southern lobe located over the UK, it significantly affects precipitation in the Mediterranean, particularly Italy and the Balkans (correlations of up to 0.6). During high SNAO summers, when strong anticyclonic conditions and suppressed precipitation prevail over the UK, the Mediterranean region instead is anomalously wet. This enhanced precipitation is related to the presence of a strong upper-level trough over the Balkans—part of a hemispheric pattern of anomalies that develops in association with the SNAO—that leads to mid-level cooling and increased potential instability. Neither this downstream extension nor the surface influence of the SNAO is captured in the two CMIP3 models examined (HadCM3 and GFDL-CM2.1), with weak or non-existent correlations between the SNAO and Mediterranean precipitation. Because these models also predict a strong upward SNAO trend in the future, the error in their representation of the SNAO surface signature impacts the projected precipitation trends. In particular, the attendant increase in precipitation that, based on observations, should occur in the Mediterranean and offset some of the non-SNAO related drying does not occur. Furthermore, the fact that neither the observed SNAO nor summer precipitation in Europe/Mediterranean region exhibits any significant trend so far (for either the full century or the recent half of the record) does not increase our confidence in these model projections.

Keywords Summer NAO · Summer Mediterranean precipitation · CMIP3 models · Projected drying · NAO teleconnections · Model projections · Observed precipitation trends

1 Introduction

Climate simulations for the twenty-first century project pronounced precipitation decreases in Europe and in the Mediterranean region, particularly in summer (Meehl et al. 2007). This projected summer drying is quite consistent across models, which makes this projection particularly compelling, but this agreement says nothing about the realism of the mechanisms involved. One way to increase our confidence in these model predictions is to investigate whether the large-scale dynamical mechanisms that influence summer precipitation in Europe and in the

I. Bladé (✉) · D. Fortuny
Facultat de Física, Departament d'Astronomia i Meteorologia, Universitat de Barcelona, c/Martí i Franqués 1, 08028 Barcelona, Spain
e-mail: ileanablade@ub.edu

B. Liebmann
NOAA/Earth System Research Laboratory, CIRES Climate Diagnostics Center, Boulder, CO, USA

G. J. van Oldenborgh
Royal Dutch Meteorological Institute, De Bilt, Netherlands

Published online: 25 November 2011

Mediterranean region are well represented in the models. Conceivably, the agreement between models could be partly due to either unrealistically strong or weak links between the large-scale circulation and precipitation. One good candidate for close examination, in so far as it drives a large fraction of the interannual variability in this sector and may thus play an important role in generating long-term changes in precipitation in observations and in the models, is the summer North Atlantic Oscillation (SNAO).

Although the NAO, understood as a seasonally-migrating surface pressure dipole over the North Atlantic region, is the most prominent regional pattern of sea level pressure (SLP) variability in every month of the year and the only pattern to be found year-round (Barnston and Livezey 1987; Portis et al. 2001), its summer manifestation (or SNAO) has received relatively little attention. For instance, scarce reference is made to the SNAO in Hurrell et al. (2003, 2009) review papers, except to say that its amplitude and spatial extent are smaller than in winter and its signature is displaced significantly northeastward. There is also some apparent ambiguity about the actual position of the SLP dipole. Portis et al. (2001) identified a summer NAO with centers of action located over the western North Atlantic ($\sim$60°W) and straddling the 50°N latitude, in contrast with the pattern in Hurrell et al. (2003), which features a dipole centered about 40° farther east, with the southern lobe positioned at 50°N. As discussed by Folland et al. (2009), this discrepancy results from the fact that Portis et al. (2001) used fixed geographical boxes (with the southern box located south of 45°N) to identify points with maximum anti-correlation on each month (the centers of action of their "mobile" NAO). Another confusion arises from the fact that some authors use a station-based definition of the summer NAO (e.g., Sun et al. 2009), even though the correlation between SLP over Gibraltar and Reykjavik drops to values less than 0.1 in summer (not shown).

Recently, Folland et al. (2009, hereafter F2009) examined many aspects of the SNAO, including its temporal evolution and surface impacts. The emphasis in that paper was placed on northwest Europe where the influence of the SNAO is strongest. They conclude that the SNAO greatly affects temperature and precipitation in this region, where summers with high SNAO indices (high pressure over the British Isles) tend to be warm and dry. They also showed that the SNAO (and its impacts over England) can be traced via proxy records all the way back to the eighteenth century. Additionally, they found the SNAO to be well-reproduced in two Hadley Centre models and that both models predict a strong upward SNAO trend in the twenty-first century, implying a progression towards quasi-permanent drought conditions in summer in northwest Europe. The impacts over the Mediterranean were less extensively studied, as the correlations between the SNAO and rainfall—indicative of wet conditions during the positive phase of the SNAO—were found to be weak (for the entire twentieth century).

As for the dynamical mechanisms behind the SNAO, Feldstein (2007) investigated the life cycle of positive and negative events and concluded that, as in winter, the SNAO is driven by both high- and low-frequency transient eddies and that wave-breaking is strongly implicated in the development of the associated upper-level anomalies, although the intensity of the breaking is weaker than in winter.

Since we wish to examine the influence of the SNAO on Mediterranean precipitation in model simulations compared to observations, we begin by revisiting the F2009 work, using updated SLP and precipitation data and focusing on that region. We extend their study by examining the robustness of the SNAO pattern, the recent SNAO trend and the associated impacts over the Mediterranean—all of which are important to assess the degree of realism of the models. In particular, our results indicate that, for the second part of the twentieth century, the relationship between the SNAO and Mediterranean precipitation is stronger than in F2009. This linkage should be well captured by the models if their projections for precipitation are to be believed, especially if the SNAO responds to increases in greenhouse gases, as suggested by F2009. We then examine long-term variations of precipitation in this region and assess to what extent they are driven by the SNAO. In addition, we investigate the dynamical mechanisms responsible for inducing a precipitation response in a region (the Mediterranean) that is not under the direct influence of the SNAO pressure anomalies.

The final part of the paper is devoted to evaluating the realism of the connection between the SNAO and Europe/Mediterranean precipitation in two global climate models (the HadCM3 and the GFDL-CM2.1 models). A subsequent paper will examine the performance of all CMIP3 models with regards to the SNAO, but for now we have chosen two models that predict strong future upward SNAO trends to illustrate potential problems related to model errors. The finding that the models are deficient in reproducing the observed relationship has important implications for the magnitude of the projected drying in the Mediterranean region.

2 Observational data

We employ a variety of state-of-the-art datasets (updated whenever possible to the summer of 2010) with the aim of testing the reproducibility and robustness of our results. Analyses for the period 1950–2010 are based on NCEP/

NCAR reanalysis data (SLP, geopotential height, lifted index; Kalnay et al. 1996) and 0.25° × 0.25° gridded E-OBS (version 3.0) precipitation and temperature data, which represent the most complete European climate dataset to date (Haylock et al. 2008). The results for this period are compared with those for the entire twentieth century using observed SLP data from the Trenberth dataset (1899–2010; Trenberth and Paolino 1980) at 5° × 5° resolution. For this long period we also use the recently released GPCC V5 0.5° × 0.5° dataset that extends from 1901 to 2009 (Rudolf and Schneider 2005). Although the results will not be presented here, the UEA-CRU (1901–2006; Mitchell and Jones 2005) and Hulme (1900–1998; Hulme et al. 1998) precipitation datasets and the EMULATE SLP dataset (1881–2003; Ansell et al. 2006) were also used to validate our results. None of our findings are sensitive to the dataset employed, except for minor differences. The summer NAO CPC index (used for comparison) and other teleconnection indices are taken from the CPC website (www.cpc.ncep.noaa.gov/data/teledoc/telecontents.shtml). Finally, high-resolution (0.25° × 0.25°) blended GHRSST daily sea surface temperature (SST) data from NOAA-NCDC were also employed (Reynolds et al. 2007).

July–August (JA) mean anomalies are computed by subtracting the corresponding climatological long-term mean. The statistical significance of correlation and regression coefficients and linear trends is estimated using a two-tailed Student-*t* test.

3 The summer NAO

The SNAO can be defined, in analogy with its winter analog, as the leading EOF of summer mean (June–August) SLP in the North Atlantic sector (Hurrell et al. 2003; see their Fig. 6). Two recent papers, however, have expressed concerns about this definition. Greatbatch and Rong (2006) examined differences between SLP reanalysis and instrumental data and concluded that, to avoid discontinuity problems with the reanalysis products in Northern Africa, the domain used in the definition of the SNAO should be restricted to the region north of 40°N. They proposed the domain [40°N–70°N; 90°W–30°E] instead of the traditional region used by Hurrell [20°N–70°N; 90°W–40°E]. Additionally, F2009 suggested excluding the month of June from the definition of the summer NAO, arguing that the temporal behavior of the June NAO differed substantially from that in July and August. A straightforward justification for restricting the analysis to the "high summer" months in our case is that, while the July and August leading SLP EOFs, calculated separately, are very similar to each other (the spatial anomaly correlation, r_s, is $\sim$0.95), the corresponding June pattern is quite different, exhibiting a southern lobe significantly displaced to the southwest (not shown).[1] For the above reasons we have opted to use the smaller domain and exclude June from the analysis.

In this paper the SNAO is thus defined as the leading EOF of July–August mean SLP in the domain [40°N–70°N; 90°W–30°E], computed for the 1950–2010 period (the period common to the Trenberth, NCEP and E-OBS datasets). We emphasize, however, that the results presented here are not sensitive to any of these choices. In particular, the pattern and time series of the SNAO as defined here are very similar to those obtained using the wider domain or the conventional summer definition,[2] apart from differences in the percent of variance explained. Even using a domain as large as [20°N–90°N, 90°W–60°E] produces essentially the same pattern ($r_s = 0.97$). Our SNAO is also reasonably well correlated ($r_t = 0.72$) with the July–August mean NAO from the Climate Prediction Center (CPC), which is based on a rotated EOF analysis of 700 hPa geopotential height for individual months (Barnston and Livezey 1987). We have also verified that the surface impacts of the SNAO (Sect. 4) are qualitatively similar regardless of the definition used. On the other hand, our SNAO is not correlated with the July–August average of either of the two station-based NAO indices (Jones et al. 1997), for reasons that will become immediately obvious. Thus our findings will bear no relation to those of studies that have used these station-based NAO definitions (e.g., Sun et al. 2009).

Our summer NAO, displayed in terms of SLP anomalies regressed upon the normalized leading EOF time series, is virtually identical in the NCEP and Trenberth datasets and explains equal fractions of variance (Fig. 1a, b; $r_t = r_x = 0.99$). This mode is well separated from the second EOF, accounting for almost twice as much variance (not shown). In its positive phase, this pattern is characterized by decreased pressure over Greenland and increased pressure in northwestern Europe, with maximum positive anomalies over the British Isles. Thus, compared to its winter counterpart (Fig. 1h), the summer NAO is displaced northeastward, is more zonally and meridionally confined and the lobes exhibit a more southwest-to-northeast orientation, with more meridional advection over Northern Europe. The

[1] The spatial correlation between the June pattern and the July/August patterns is $r_s \sim 0.65$ for the 1950–2010 period; the correlation using the June EOF-2 is even lower. An SNAO-like EOF is also not found in September.

[2] The spatial (temporal) correlation r_s (r_t) is 0.98 (0.92) and 0.94 (0.86), respectively, when computed for the 1950–2010 period. The resemblance can be verified by comparing Fig. 1a, b, d to fig. 6 in Hurrell et al. (2003), which shows the leading EOF of JJA SLP computed over the wider domain for the 1899–2001 period—although the southern lobe is centered west of the British Isles rather than right over them.

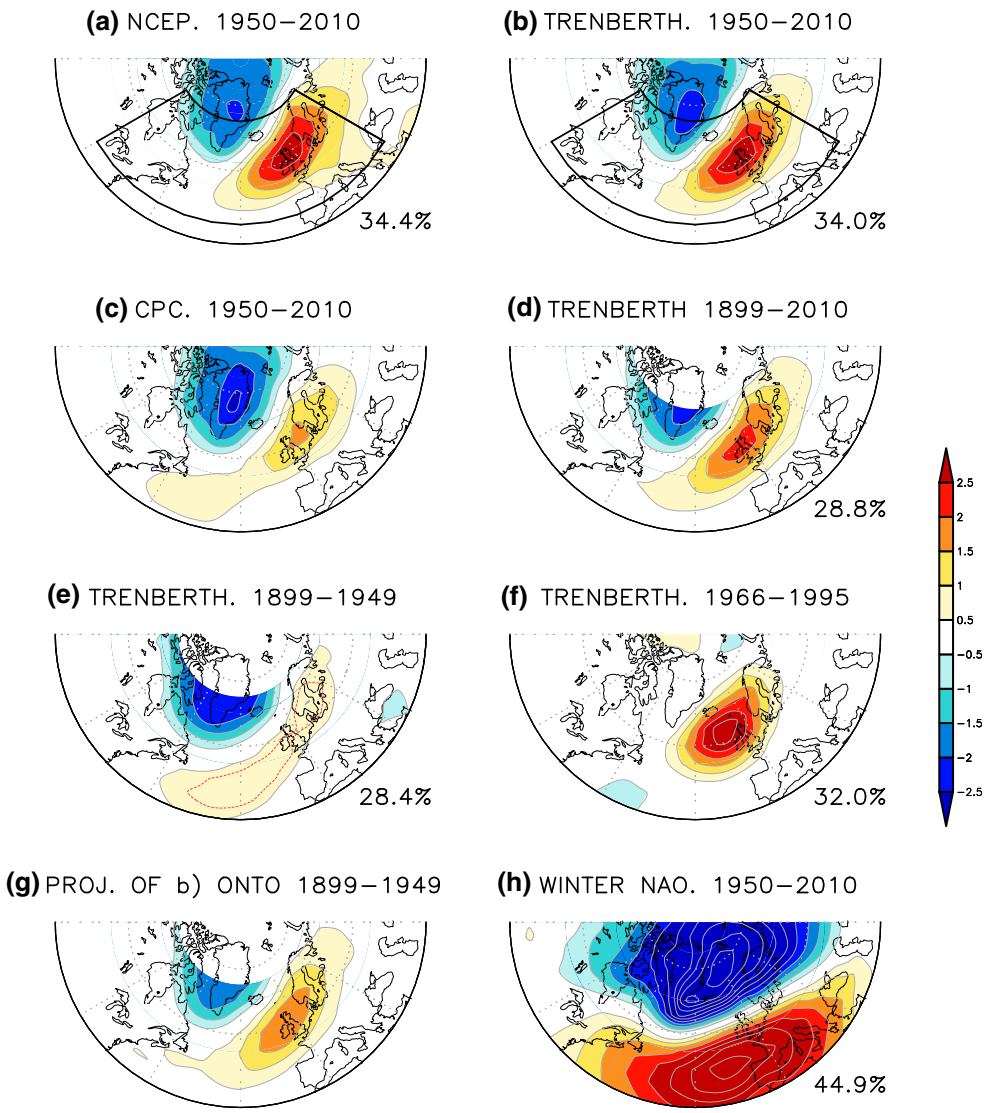

Fig. 1 *Top panels*: Spatial pattern of the summer NAO defined as the leading EOF of July–August mean SLP in the domain (40°N–70°N; 90°W–30°E; see *black box*), based on the NCEP (**a**) and Trenberth (**b**) datasets, for the baseline period 1950–2010. The EOFs are displayed in terms of regressions between the normalized time series of the EOF and SLP anomalies at every grid-point (the anomalies shown thus correspond to a standard deviation of the SNAO time series). Contours are 0.5 hPa. The percent of variance explained by the EOF is indicated next to each panel. **c** Regression of mean July–August SLP, for the 1950–2010 period, onto the normalized July–August mean CPC NAO index. **d**–**f** Same as **b** but for different periods. In **e** the 0.75 hPa contour is also shown (*dashed red line*). Note that, prior to 1946, the Trenberth dataset does not cover the region north of 70°N (hence the blank region in polar latitudes). **g** Regression of mean July–August SLP, for the 1899–1949 period, onto a normalized "projected" SNAO index obtained by projecting the SNAO "baseline" pattern (**b**) onto the SLP field. **h** Same as **b** but for the winter-mean (DJF) NAO, defined as the leading EOF of SLP in the same domain

corresponding regressed anomalies are also weaker. The poleward shift in the location of the centers of action relative to winter explains the lack of correlation with the station-based (Iceland and either Azores or Gibraltar) NAO indices of Jones et al. (1997). The resemblance with the CPC-NAO can be seen in Fig. 1c, which displays regressions of SLP onto the normalized July–August mean NAO-CPC index, although it should be noted that for the CPC-NAO pattern the southern center of action is weaker.

This NAO pattern is also well-reproduced when using data for the full 1899–2010 period, but for a slightly weaker southern lobe (Fig. 1d). This is consistent with the results of F2009, who computed the SNAO with a different SLP dataset but for a similar period (1881–2003, EMULATE dataset; their fig. 1b[3]). For the first half of the century (1899–1949), however, the southern lobe is much fainter (Fig. 1e; note the additional dotted 0.75 hPa contour).

[3] Note that in Folland et al. (2009) the anomalies in fig. 1 are normalized regressions weighted by the square root of the cosine of latitude (S. Ineson 2010, personal communication), which explains the difference in magnitude between their fig. 1b and our Fig. 1d.

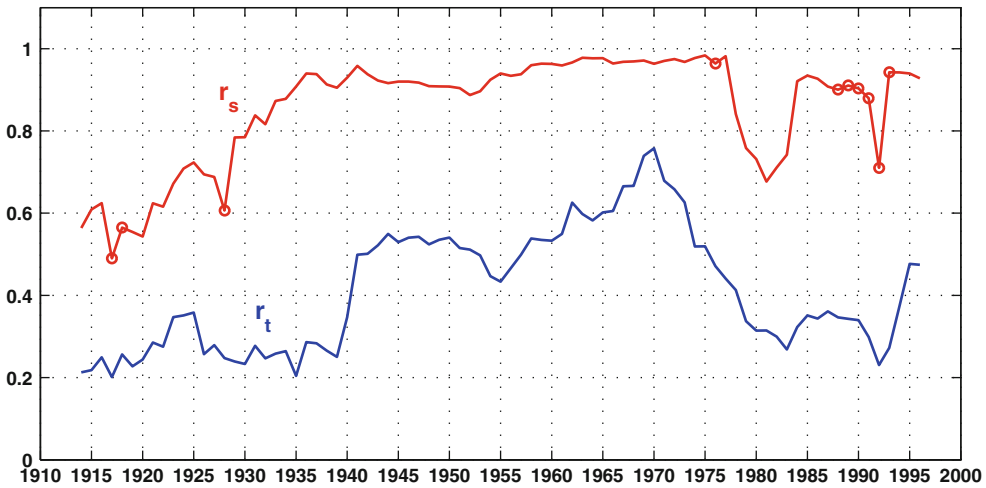

Fig. 2 30-Year running-mean EOF analysis for the 1899–2010 period, where the time axis indicates the window center year. The *red curve* is the running-mean anomaly spatial correlation (r_s) between the "baseline" regressed SNAO pattern (computed for the 1950–2010 period, i.e., pattern in Fig. 1b) and the corresponding SLP regression obtained using the 30-year leading EOFs. The *red circles* indicate periods in which the leading EOF is not well separated from the second EOF. The *blue curve* is the running-mean temporal correlation (r_t) between the two centers of action of the baseline pattern

Furthermore, the anti-correlation between the two centers of action, [10°W, 55°N] and [40°W, 70°N]—a measure of the strength of the sea level pressure seesaw between Greenland and the UK—drops from 0.52 for the 1950–2010 period to 0.23 for the 1899–1949 period.

To examine the robustness of this summer NAO pattern, we computed the leading EOF for a 30-year running window between 1899 and 2010 and plotted the spatial anomaly correlation (r_s) between each of these EOFs and the corresponding pattern for the 1950–2010 period, or "baseline" SNAO pattern (Fig. 2). Also shown in this figure is the running-window temporal correlation (r_t) between the two centers of action. The SNAO emerges as the preferred pattern of variability between about 1935 and 1975 ($r_s > 0.9$), with a relatively strong seesaw ($r_t > 0.5$). Prior to that, the leading pattern resembles the less distinct dipole in Fig. 1e, with very feeble anomalies over the UK, and a weak seesaw ($r_t < 0.3$). This result is consistent with Greatbatch and Rong (2006), who noted a large drop in the correlation between the SNAO index and central England temperatures between 1910 and 1930. Since 1975, the seesaw has also been less active and the SNAO has been less consistently dominant, so that in some 30-year periods it does not emerge as the leading mode of variability, or else it is not well separated from the second EOF, according to the criterion of North et al. (1982; see red circles in Fig. 2). When absent as EOF-1 (e.g., for the 30-year period centered on 1981), the SNAO is replaced by a single anomaly over the UK that extends into Iceland, where the node of the "baseline" SNAO lies, maintaining the blocking aspect intact (Fig. 1f).

The change in the SNAO around 1940 could be connected to a change in the observing system.[4] However, even disregarding the results for the first part of the century, where data quality or missing data may be an issue and where even the winter NAO is absent during certain 30-year periods (not shown), it is clear from our analysis that the summer NAO is a less robust and prominent feature of the atmospheric circulation than its winter counterpart, with periods of reduced activity and a weaker dipole (for the winter NAO the anti-correlation between centers of action is −0.78 for the 1950–2010 period, compared to −0.52 for the SNAO).

The above results justify our choice of a definition for the SNAO that avoids the questionable first part of the record and ensures that results for the 1950–2010 period will be the same regardless of whether the NCEP or Trenberth SNAO index is used. To examine the impacts of the SNAO during the entire record, we will construct an SNAO index for the full period by projecting the SNAO "baseline" pattern onto the SLP field over the SNAO domain.[5] Nevertheless, it is important to keep in mind that

[4] For instance, the GHCN database contains only three Greenland stations with 40 years or more of data in the period 1899–1949, but none of them has 40 years of data in the period 1950–2010.

[5] For the 1950–2010 period, this projected SNAO index coincides, of course, with the time series (PC) of the leading EOF for that period (or baseline pattern). For the entire 1899–2010 period, the projected index is correlated at 0.98 with the PC of the leading EOF for that period (Fig. 1d). For the early period (1899–1949), however, the correlation with the PC of the leading EOF (Fig. 1e) is only 0.76.

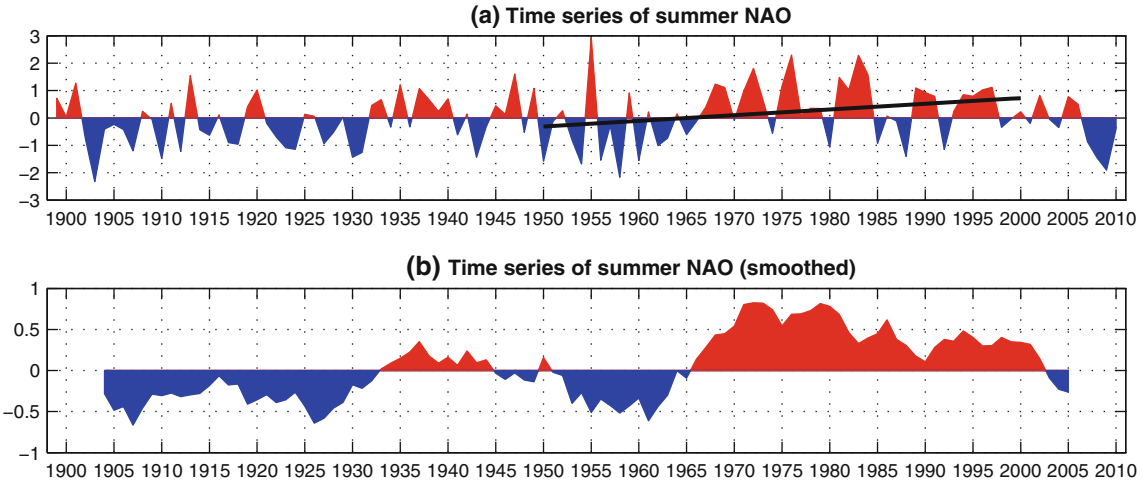

Fig. 3 **a** Normalized index or time series of the SNAO obtained by projecting the SNAO "baseline" pattern (period 1950–2010) onto the Trenberth SLP field for the full 1899–2010 record. The *black line* denotes the 1950–2000 trend highlighted by HF2002. **b** Same but smoothed with an 11-year running-mean (note that scale of the y-axis is different)

for the early part of the record the associated regressed anomalies are weaker (Fig. 1g).

The time evolution of the SNAO is shown in Fig. 3, using this normalized projection of the SNAO pattern onto the Trenberth SLP field for the entire period. The lower panel shows the smoothed evolution using an 11-year running mean. While the fluctuations of the SNAO are dominated by variability at the interannual timescale (the lag-1 autocorrelation is ~ 0.1), there is also substantial variability on multi-decadal timescales, with the SNAO tending to exhibit a preferred phase for years at a time. Feldstein (2007) has speculated that slowly evolving changes in the stretching deformation field in the vicinity of the North Atlantic jet could explain this sustained predilection for one phase.

The latest of these multidecadal swings occurred around 1967 and was described by Hurrell and Folland (2002, hereafter referred to as HF2002) as a "change towards persistent anticyclonic flow" in northern Europe. The 30-year period after 1967 was indeed characterized by an unprecedented frequency of summers with large positive SNAO indices compared to the previous instrumental record. In the last decade, however, the tendency for the SNAO to reside in the positive phase has dwindled, with large negative values for the past four summers (2007–2010; Fig. 3a). This recent behavior of the SNAO calls into question the existence of a permanent shift towards a positive state or a true long-term trend (HF2002). Indeed, while at the time of that study the SNAO trend was statistically significant, in both datasets and for both the entire century and the second half, the current updated trend no longer is (Table 1; see also past trend line in Fig. 3a).[6] Neither is the corresponding trend of SLP averaged over the southern center of action of the SNAO, which is the index actually considered by HF2002 (not shown). Greatbatch and Rong (2006) also pointed out that the upward SNAO transition in the 1960s was simply part of the low-frequency oscillatory character of the SNAO. The issue is reminiscent of the large positive excursion of the winter NAO in the 1990s (Hurrell 1995), which has also reversed since then. On the other hand, F2009 concluded, based on a tree-ring reconstruction, that the high positive values of the SNAO index circa 1970–1995 were unprecedented in the past three centuries. We will return to the issue of trends in Sect. 5.

Table 1 Trends in the SNAO index for two datasets and various periods (for the Trenberth dataset, the index for the first half of the record is obtained as a projection of the baseline pattern, see text)

Dataset	Trend until year 2000 (SD/century)	Trend until year 2010 (SD/century)
NCEP (1950-)	2.52**	0.92
TRENBERTH (1950-)	2.07*	0.43
TRENBERTH (1899-)	0.93**	0.54

Middle column indicates trends up to 2000 since 1950 and since 1899. Last column indicates the same trends updated to 2010. Units are standard deviation (SD, computed for the full record of each dataset) per century. Trends that exceed a two-tailed Student-*t* test at the 95% (99%) level are indicated with one (two) *asterisks*. Note that the trends need to be expressed in terms of SD of the index time series (PC) because non-normalized trends cannot be directly compared across datasets with different spatial resolutions (as is the case for the Trenberth and NCEP datasets)

4 Impacts of the SNAO on Mediterranean surface climate

We now consider the influence of the SNAO on European climate, with emphasis on precipitation in the Mediterranean

[6] See Liebmann et al. (2010) for a method to illustrate the sensitivity of trends to end points.

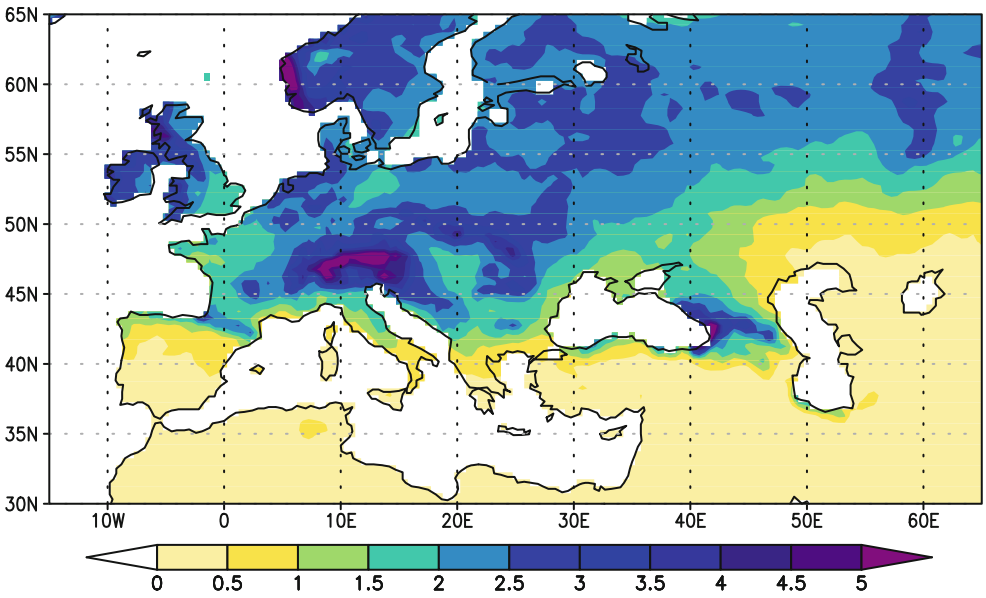

Fig. 4 Climatological (1950–2009) July–August mean precipitation in Europe in mm/day. GPCC v5 data are used in this figure in order to include results over Northern Africa where E-OBS data are scarce

region. To provide context for the results, we first show the climatological summer precipitation (Fig. 4). The regions south of about 42°N receive less than 1 mm/day on average, which, in the eastern Mediterranean, is consistent with strong mean subsidence (Rodwell and Hoskins 1996). Southern France, northern Italy and the Balkans, however, are as wet as parts of the UK. Even where precipitation is scarce it is important to understand the dynamical mechanisms that drive year-to-year fluctuations and may lead to persistent changes in the future.

We now begin our analysis by computing linear correlations between the SNAO index and surface temperature and precipitation for the period 1950–2010, using E-OBS data (Fig. 5, left panels), and comparing them to their winter counterparts (right panels).[7] Summers with a positive SNAO index tend to be characterized by warm and dry conditions in southern Scandinavia and northwest Europe, particularly the British Isles, and cold and wet conditions in the northeast Mediterranean (Italy, the Balkans and western Turkey), as well as wet anomalies in central Iberia. These results are consistent with F2009 and Mariotti and Arkin (2007), except the correlations found here are somewhat stronger. Chronis et al. (2011) also find strong negative temperature-SNAO correlations in Greece in August, indicative of cooler than normal conditions during summers with high SNAO, which they attribute to enhanced northerly Etesian winds and cloudiness.

The precipitation correlation pattern in summer is broadly opposite in sign, and comparable in strength, to the corresponding winter pattern (Fig. 5b). In northern Europe, this sign reversal is consistent with the seasonal changes in the NAO circulation pattern (cf. Fig. 1a, b, h). That is, during winters with a positive NAO, eastward advection of moist maritime Atlantic air enhances precipitation in that region (particularly along the western coasts and on the upwind side of mountain ranges), whereas the anticyclonic conditions that prevail there during positive NAO summers tend to suppress precipitation. Over the Mediterranean, however, the sign switch in the impact of the NAO from winter to summer is less straightforward. The SNAO is too far north to directly modulate the inflow of maritime air into southern Europe; moreover, if anything, this effect would lead to correlations of the same polarity as in winter. Thus, the positive summer precipitation correlations in the northern Mediterranean region, particularly Italy and the Balkans, are surprising. The magnitude of the correlations, however, is weaker than in winter and also weaker than in northern Europe (maximum correlations of 0.6 vs. 0.8), which raises the question of the robustness of the results.

Consequently, we verified that the results in Fig. 5a were reproducible when using other datasets and extending the analysis to the entire century. For instance Fig. 6 shows the *regressions* between the SNAO index and GPCC precipitation for the early and late parts of the record. The results confirm the existence of a widespread pattern of positive precipitation anomalies, centered in the Balkan/Italy region and extending to Iberia, Turkey and parts of northern Africa, during summers in which the SNAO is in the positive phase (Fig. 6a). However, and consistent with the weaker expression of the SNAO in the first half of the twentieth century (Fig. 1g), the precipitation pattern is

[7] Almost identical results are obtained when data are detrended prior to the regression calculations, consistent with the weak SNAO trend.

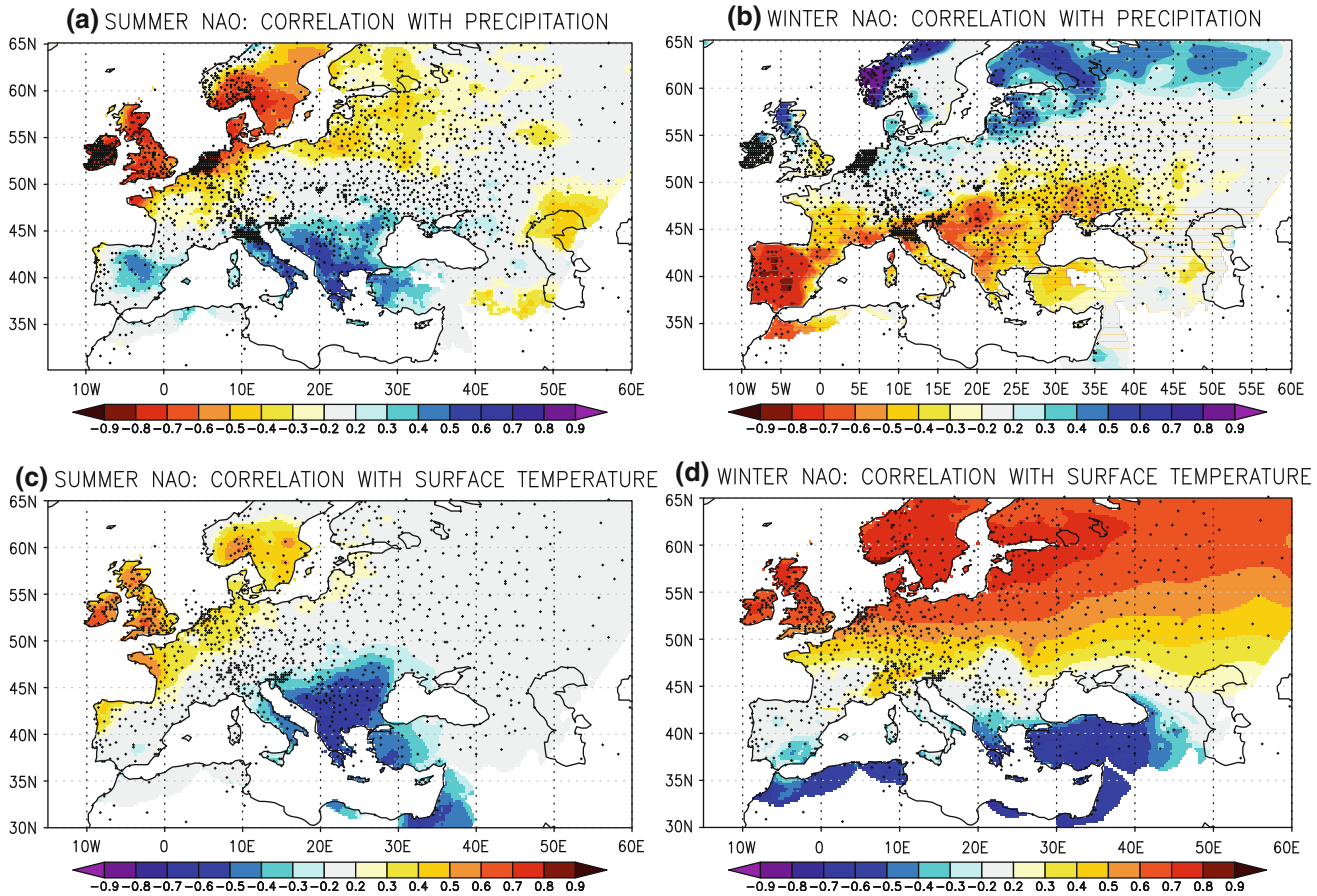

Fig. 5 *Left panels*: correlation between the summer (JA) NAO index (Trenberth dataset) and precipitation and surface temperature (E-OBS data) for the 1950–2010 period. Shading interval is 0.1. Areas shaded in grey indicate correlations smaller than 0.2, which do not pass a two-sided Student-t significance test at the 90% level. Areas with missing data are left blank. Station locations for each dataset are indicated by a dot. Note the reversed colorbar for precipitation, so that *red shading* indicates dry or warm anomalies whereas *blue shading* indicates wet or cold anomalies. *Right panels*: same for the winter (DJF) NAO

substantially weaker and less significant for the early record, particularly in the Mediterranean and eastern Europe (Fig. 6b). Some of these differences may be related to the scarcity of observations in these regions prior to 1930 (not shown) and may not reflect a real change in the impact of the SNAO. (Note that to minimize the risk of spurious differences in very dry areas, regions with less than 5 mm/month precipitation are hatched, following Obregón et al. 2010). Regardless, these differences explain why, in F2009, the SNAO correlations with cloudiness, available only since 1954, are stronger than the correlations with precipitation, which were computed for the entire century. As a final check, we verified that the correlation pattern for individual July and August months was the same as that obtained using JA averages (not shown). An independent verification of our results is also provided by Feidas et al. (2007) and Hatzianastassiou et al. (2008) who find correlations of about 0.4–0.5 between an index of the summer NAO and mean precipitation over Greece, estimated from rain gauge station data and satellite data, respectively.

It is interesting that the pattern of precipitation anomalies associated with the SNAO highly resembles the leading EOF of JA mean precipitation in Europe (11°W-35°E; 35°N-65°N), shown in Fig. 7a using GPCC data, which explains 18% of the total variance and whose time series is in turn very well correlated with the SNAO ($r_t = 0.87$ for the second half of the century and 0.82 for the entire record). A similar result has been obtained by Zveryaev and Allan (2010) for the 1979–2006 period. That this EOF truly represents a physical pattern of spatially coherent rainfall fluctuations, with out-of-phase variations in northern and southern Europe, can be confirmed by computing one-point correlation maps for precipitation in individual regions (e.g., Fig. 7b, computed for an eastern Mediterranean box, using E-OBS data for independent verification).

In summary, the summer NAO produces a robust broad-scale pattern of precipitation anomalies in the Mediterranean, with enhanced rainfall during its positive phase, particularly Spain, Italy and the Balkans. This pattern is the

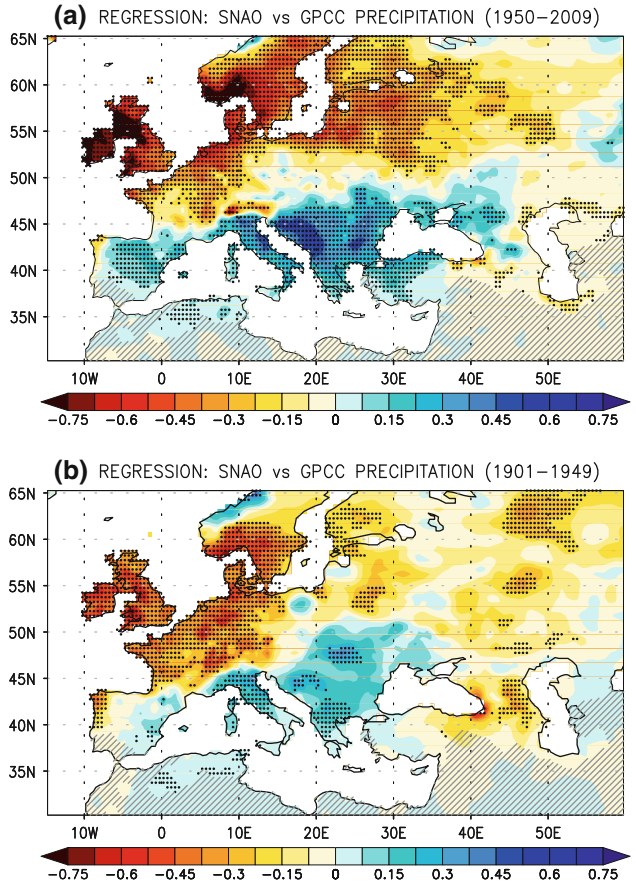

Fig. 6 Regressions between the normalized summer (JA) NAO index and GPCC precipitation for the 1950–2009 period (*top*) and the 1901–1949 period (*bottom*). Shading interval is 0.075 mm/day. Regressions that pass a two-sided statistical test at the 95% confidence level are marked with a *black dot*. In this and subsequent figures, areas where climatological-mean JA precipitation is less than 5 mm/month (for the 1950–2009 period and the respective dataset) are hatched and statistical significance is not plotted

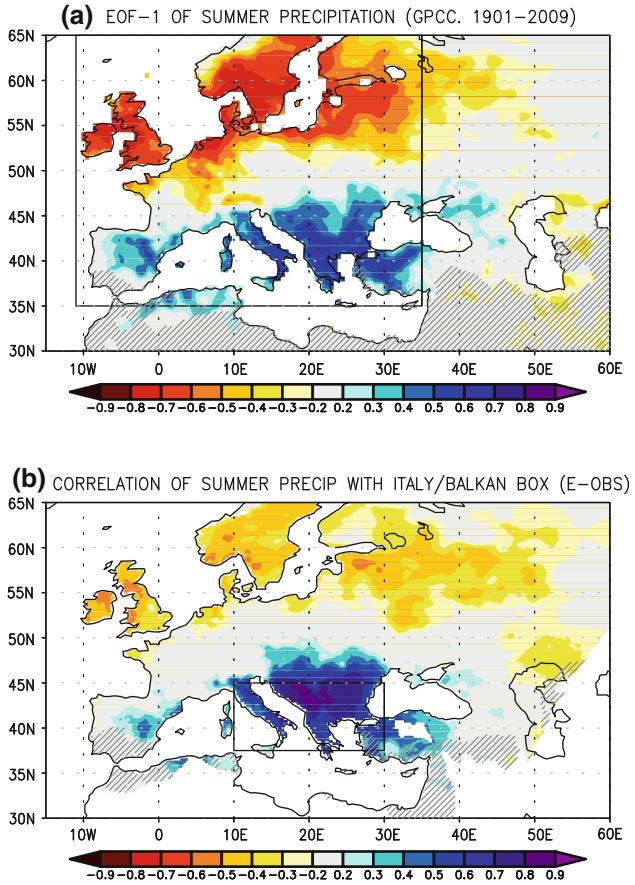

Fig. 7 **a** Leading EOF of mean July–August precipitation in the European/Mediterranean region (11°W–35°E, 35°N–65°N; see *box*), expressed in terms of correlations between the time-series of EOF-1 and precipitation at each grid-point. Data is GPCC (1901–2009). Shading interval is 0.1. Areas shaded in *grey* indicate correlations less than 0.2, which corresponds approximately to the two-sided 95% confidence level. Hatching as in Fig. 6. **b** Correlation between precipitation averaged over the eastern Mediterranean (Italy/Balkans, 10°E–30°E, 37.5°N–45°N; see *box*) and precipitation at every grid-point for the 1950–2010 period (E-OBS data). Plotting convention same as in panel (**a**). *White areas* indicate missing data

strongest of all signals between known (CPC) summer teleconnection patterns and precipitation in this sector (not shown). Although modest ($r < 0.6$), these correlations are important in modulating summer precipitation totals in these areas. We will address the issue of the mechanism responsible for this influence in Sect. 6.

5 Decadal modulation of Mediterranean precipitation by the SNAO and trends

Since the SNAO varies on multidecadal scales (Fig. 3), it may be expected to modulate Mediterranean precipitation on these long timescales also. This modulation can be examined by plotting the time series of summer precipitation averaged over the Italy/Balkan region (10°E–30°E; 37.5°N–45°N; see box in Fig. 7b), together with the time series of the SNAO (Figs. 8a-b). Because the precipitation areal averages obtained using GPCC and E-OBS data are correlated at 0.98, for this figure we have used GPCC data, updated to 2010 with the corresponding E-OBS value (adjusted for differences in the mean over the 1950–2000 period). The figure shows that the impact of the SNAO on Mediterranean precipitation is quite linear, with large positive rainfall anomalies during summers in which the SNAO is high (see also scatter plot in Fig. 8d). This is in contrast with Mariotti and Arkin (2007), who report only a modest enhancement of precipitation during the positive SNAO phase. Note however that their result is based on NCEP reanalysis precipitation; other sources of discrepancy may be their use of the CPC NAO index and June-July–August (JJA) averages.

The strengthening of the relationship between interannual variations in the SNAO and precipitation in the Italy/

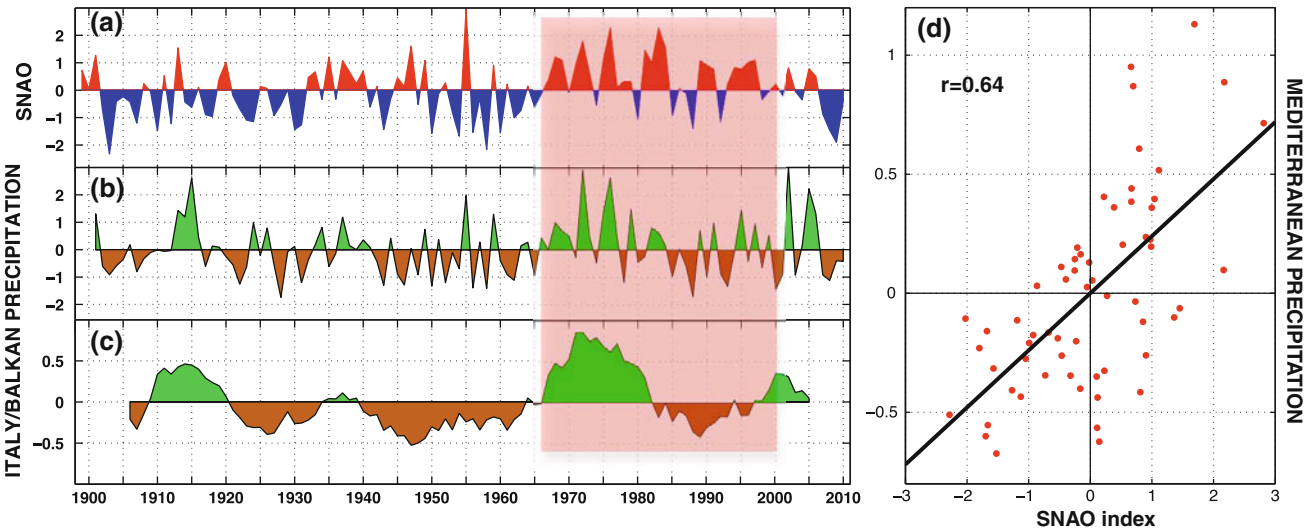

Fig. 8 **a** Time series of the normalized July–August SNAO index (*top panel*, same as Fig. 3a). **b** Time series of the normalized July–August mean precipitation averaged over the Italy/Balkan region (see *box* in Fig. 7b). GPCC data is used except for the 2010 value which is the EOB-S value (scaled for differences in the mean). **c** The 11-year running mean of the precipitation timeseries. The *red box* indicates the recent period where the SNAO has resided preferentially in its positive phase. **d** Scatter plot of the SNAO index and the (unfiltered) precipitation time-series (E-OBS data)

Balkan region since 1950 is also evident in Fig. 8: the correlation between the SNAO and this precipitation index is 0.67 for the 1950–2010 period but only 0.33 for 1901–1949. There is also a clear tendency for wetter summers after 1967 compared to the previous decades, concomitantly to the upward shift in the SNAO, but this tendency does not extend for as long as the positive swing in the SNAO (indicated by the red box; see smoothed precipitation curve in Fig. 8c).[8] Thus, while decadal fluctuations in summer precipitation in the Italy/Balkan region have been partly related to the SNAO, no long-term increase in precipitation accompanied the apparent upward SNAO trend that persisted until the year 2000. More generally, our trend calculations indicate that mean precipitation in this region does not appear to have varied significantly throughout the period of record, regardless of whether the whole century or the recent 1950–2010 period is considered (not shown).

We pause here to point out that the absence of significant summer precipitation trends (recent or long-term) in the Italy/Balkan region as a whole also holds true at a local level and for the entire European continent. Figure 9 shows linear trends computed for the period 1950–2010 using the E-OBS dataset and for the 1901–2009 period using the GPCC dataset. Few regions exhibit statistically significant trends in either period and even fewer exhibit significant trends of the same sign in both periods. In addition, most of the regions with statistically significant trends tend to be localized or poorly sampled regions where most of the apparent widespread significance is due to the interpolation (e.g., Turkey; see Fig. 5a for station location). Note again, however, that the assessment of long-term trends is compromised in places by the scarcity of data prior to 1930 (i.e., a lack of statistically significant trend may simply indicate lack of data). Nevertheless, even for the recent period, widespread statistically significant *reductions* in precipitation have occurred only in parts of the British Isles. The Mediterranean region exhibits weak non-significant trends of either sign, with very few exceptions. Very similar results are obtained if one considers the entire summer season (i.e., JJA means, not shown).

This conclusion is at odds with findings from some studies indicating that summer precipitation in the Mediterranean and Europe has diminished in recent years. For instance, Pal et al. (2004) document a decrease in summer precipitation over "most of Europe" between the periods (1951–1975) and (1976–2001). Giorgi and Lionello (2008) estimate this reduction to be about 4% for the Mediterranean region (28°N–48°N; 9.5°W–38.5°E), for slightly different periods ([1981–2000] minus [1961–1980]). Although both studies employ a different dataset (CRU), we have reproduced their analysis and find that very few of the differences are statistically significant at the 95% level (not shown). Moreover, for the Balkan/Italy region it is clear from Fig. 8b, c that the decrease reported in Giorgi and Lionello (2008) arises from the fortuitous choice of two wet decades followed by two dry decades. This result

[8] In a very recent paper, Mariotti and Dell'Aquila (2011) find a strong (0.79) correlation between a *detrended* JJA SNAO index and detrended mean precipitation averaged over the entire Mediterranean domain, which is not inconsistent with our undetrended results.

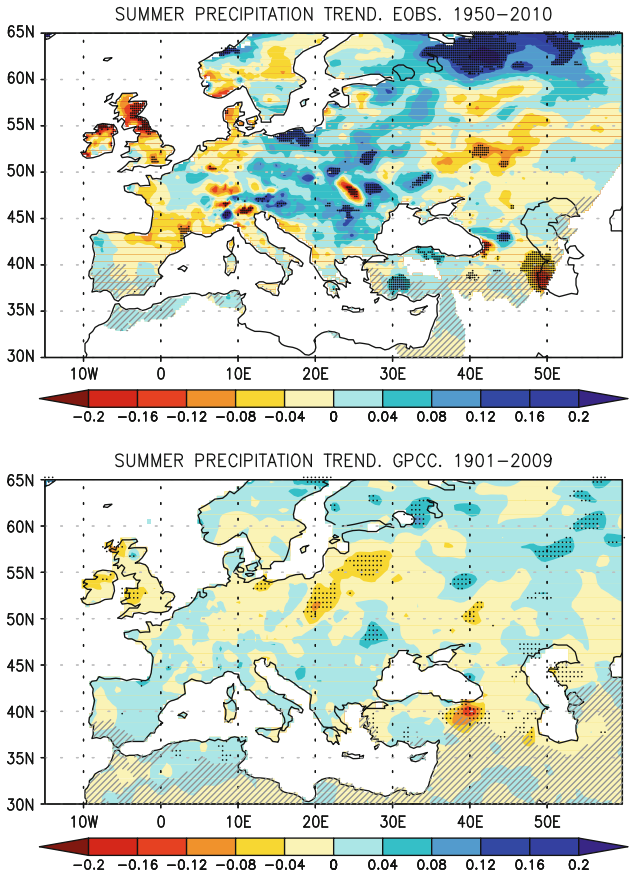

Fig. 9 *Top*: Observed summer (JA) linear precipitation trends for the 1950–2010 period computed using the E-OBS dataset. Contours are 0.04 mm/day/decade. The *black dots* indicate trends that exceed the two-sided 95% significance level. Hatching as in Fig. 6. *Bottom*: Same for the GPCC dataset and the 1901–2009 period

cautions against the use of differences between multi-decadal periods as an estimate of long-term changes in regions of strong decadal variability, as the results exhibit a poor signal-to-noise ratio. In light of the above updated trend results, we do not find evidence to support the conclusion that summer precipitation has decreased in the Mediterranean region.

6 Mechanisms for the influence of the SNAO on summer Mediterranean precipitation

As mentioned in Sect. 3, given the northern location of the southern lobe of the summer NAO, it is not readily apparent why precipitation in the Mediterranean region should be affected by fluctuations in the SNAO. The inhibited precipitation in northwest Europe during summers with a positive SNAO is of course readily attributable to the enhanced anticyclonic conditions and associated large-scale subsidence over the region. In contrast, the bland surface pressure pattern in the Mediterranean (Fig. 10a), with weak positive SLP anomalies and weak northerly flow north of the Balkans, weak offshore winds further south and easterly flow across central Italy, cannot explain the widespread increase of precipitation over the Balkans, western Turkey, Spain and Italy (although these easterly winds do advect moisture into northern Italy, so does the reverse pattern). Mariotti and Arkin (2007) find that anomalous moisture convergence accompanies the enhanced precipitation, but this anomaly also seems unconnected to the SLP pattern.

Examination of 500-hPa and 200-hPa geopotential height (Z) anomalies regressed onto the SNAO index, however, reveals a statistically significant upper level trough centered over the Balkans, overlaying the region of largest positive precipitation anomalies (Fig. 10b, c), with a second weaker trough west of Iberia. The zonal elongation of this negative Z-200 anomaly is consistent with the structure of the precipitation anomalies. Note that these troughs appear to be part of a hemispheric equivalent barotropic pattern of anomalies, reminiscent of Branstator's (2002) wave-guided circumglobal patterns. Although the two centers of action in the North Pacific are weak, the pattern strengthens considerably over North America so that the correlation between the SNAO index and this center of action exceeds 0.5 at 200 hPa (this anomaly center was also noted in F2009; their Fig. 2b). Analysis of the dynamical origin of this downstream extension of the SNAO, which is strongest at upper levels and not manifested at the surface (Fig. 10d), is beyond the scope of this paper. We simply note that, like the winter circumglobal wave, this hemispheric pattern may be due to a quasi-stationary Rossby wave excited (directly or indirectly) by the SNAO and meridionally trapped by the large vorticity gradients within the summer jet stream (Watanabe 2004). Alternatively, the SNAO could be part of a global pattern, or even originate over North America.

Regardless of the dynamical origin of the downstream pattern, the existence of upper level troughs over the Balkans, Italy and Spain can explain the influence of the SNAO on precipitation in these regions. The associated tropospheric mid-level cooling increases the potential instability of the environment, which, coupled with the low-level moisture supplied by the warm summer SSTs in the surrounding seas (not shown) and the orographic uplift provided by the mountainous terrain, constitute favorable conditions for the development of summer convection. This contention is supported by the correlation between the SNAO and the NCEP Lifted Index (a quantitative measure of potential instability, defined as the difference between the ambient temperature at 500 hPa and the temperature of an air parcel lifted adiabatically from the surface to that level), which is negative over the Mediterranean region, indicating unstable conditions during positive SNAO summers (Fig. 11a). Additionally, the fact that the

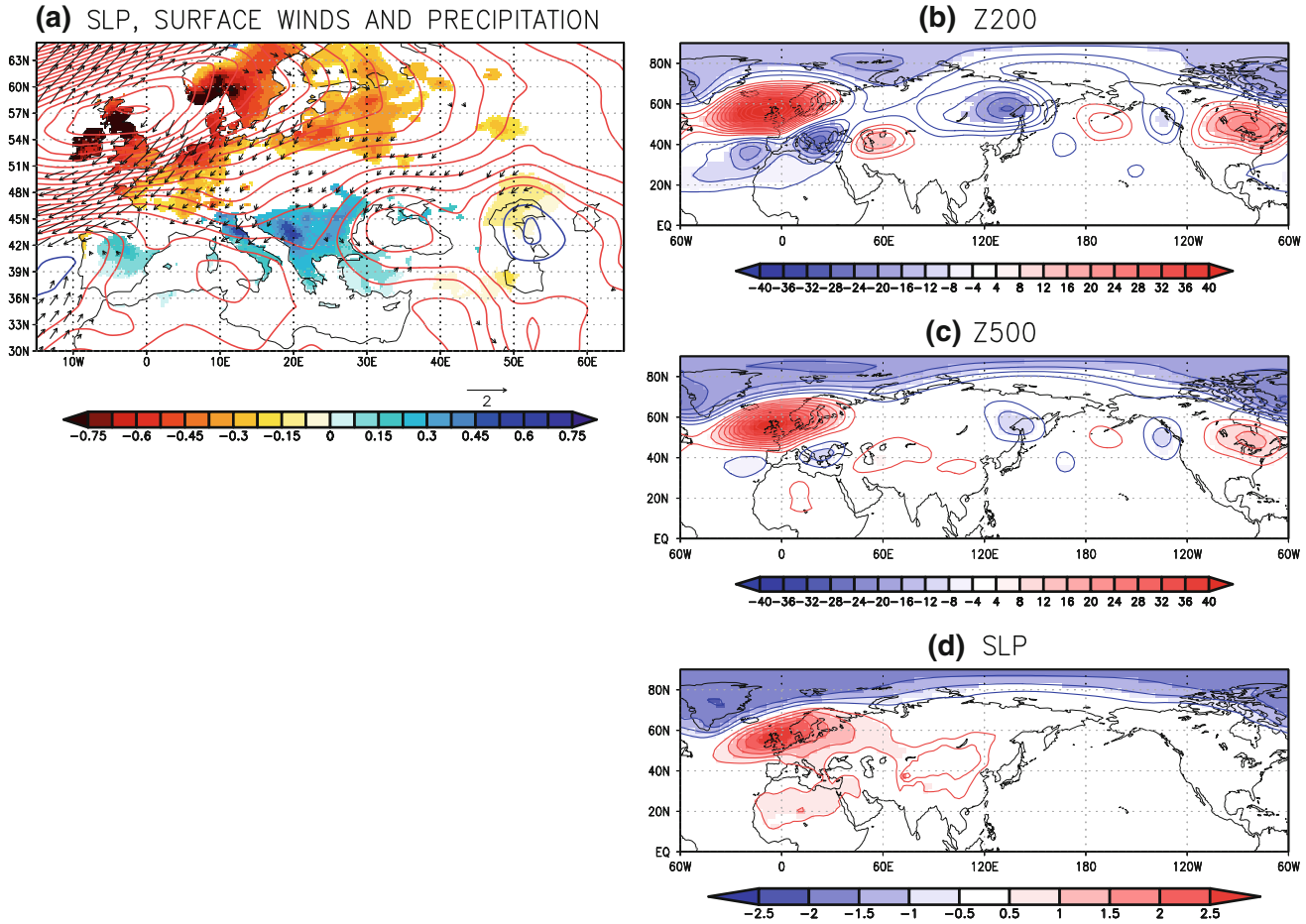

Fig. 10 *Left Panel*: Regional regressions of JA SLP anomalies (contours, contour interval is 0.15 hPa), surface winds (arrows, maximum vector is 2 m/s) and precipitation (*shading*, contour is 0.075 mm/day) onto the normalized SNAO index, for the period 1950–2010. For winds and precipitation, only regressions that exceed the two-sided 95% significance level are shown. *Right panel*: Same but for hemispheric regressions of the 200-hPa geopotential height field (*top*), 500-hPa geopotential height field (*middle*) and SLP (*bottom*). Contour interval is 4 m and 0.5 hPa, respectively. Regressions that exceed the two-sided 95% significance level are *shaded*

observed precipitation correlation pattern (Fig. 5a) is reasonably well replicated in the NCEP (Fig. 11b) or ERA-40 reanalysis (Mariotti and Arkin 2007) supports the notion that large-scale control is important in triggering local summer convection.

To assess whether these SNAO-related interannual variations in precipitation in the Mediterranean are influenced by concomitant changes in SST, we computed the correlation between the SNAO index and high-resolution satellite-derived SST data for the 1982–2010 period (Reynolds et al. 2007). Consistent with the pattern of land temperature anomalies (Fig. 5b), the Mediterranean sea tends to be anomalously cold when the SNAO is positive, particularly in the southeast and Adriatic Sea (Fig. 12; see also Chronis et al. 2011). This cooling is likely due to the integrated effects of increased cloud cover (decreased solar radiation) but it may also aid local precipitation by enhancing the land-sea thermal contrast and intensifying the local sea-breeze circulations.

Although the SNAO connection to precipitation over Italy and the Balkans is relatively modest, a correlation analysis of JA precipitation in this area with SLP and Z200 retrieves the same patterns as in Fig. 10 (not shown), indicating that the SNAO is in fact the dominant dynamical pattern that affects summer precipitation in this area. This result also suggests that trends in the SNAO will be the main dynamical driver of future precipitation trends in this region. This issue is examined in the next section.

7 The impact of the SNAO in model simulations and projections for the twenty-first century

As stated in the Introduction, the ultimate goal of our investigation is to assess the extent to which current climate models reproduce the spatial pattern and the surface impacts of the summer NAO. As a preview, in this paper we will examine the SNAO in the HadCM3 and GFDL-

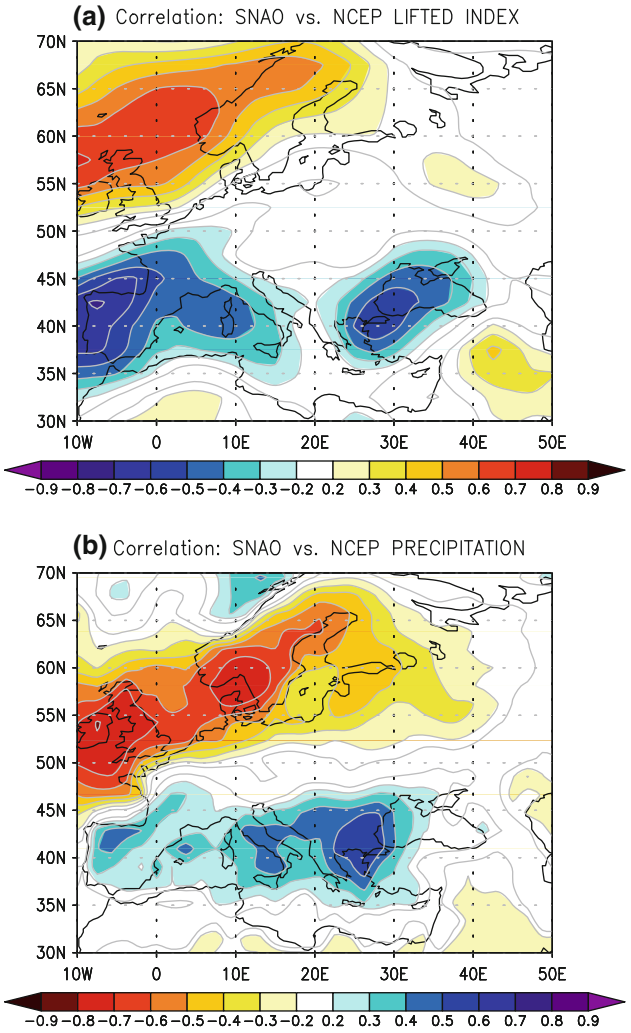

Fig. 11 Correlation between the SNAO index (NCEP) and the NCEP lifted index (*top*) and NCEP precipitation (*bottom*). Contour interval is 0.1 with correlations less than 0.2 (not significant) not shaded. Note that, as usual, the *color bar* for precipitation is reversed. A negative lifted index indicates conditional instability

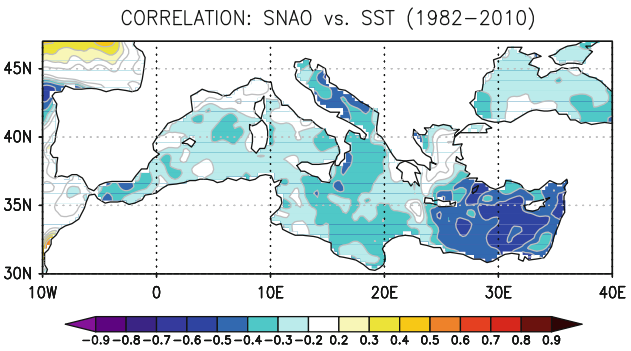

Fig. 12 Correlation between the July–August SNAO index and high-resolution SST for the 1982–2010 period. Contour is 0.1 with the first contour not shaded

CM2-1 model. The first model was already examined in F2009, but only with regards to the SLP pattern. These authors found that the SNAO was well reproduced in a control simulation of the model and was predicted to trend upwards in a transient, increased-CO2, simulation. Given that enhanced anticyclonic conditions over northern Europe must necessarily lead to decreased precipitation, they concluded that the SNAO upward trend was likely contributing to the strong predicted summer drying in that region. Based on our observational results, however, the impact of this SNAO trend on Mediterranean precipitation should be exactly opposite and could thus be expected to partially offset the drying trend due to other mechanisms not related to large-scale circulation changes, such as soil moisture feedbacks or increased land-sea temperature contrasts (Rowell and Jones 2006).

Since this issue was not addressed in F2009, we now consider the SNAO in the merged consecutive 20C3M/SRESA1B (1860–2200) simulation with the HadCM3 model that was performed as part of the Fourth Assessment Report (AR4) of the Intergovernmental Panel on Climate Change (IPCC 2007). The SNAO is computed for the same baseline period and domain as for the observations. Consistent with F2009, we find that the SNAO is well simulated, in terms of spatial pattern, percent of variance explained and magnitude of anomalies, as the leading EOF of JA mean SLP (Fig. 13a). The associated precipitation pattern, however, while qualitatively similar to the observed, with dry anomalies over northwest Europe, is far too weak in the Mediterranean region, except over Iberia (cf. Fig. 13b, c with Figs. 5a and 6a). This is consistent with the fact that, although the simulated 200-hPa height anomalies also resemble the observed pattern (Fig. 13d), the trough over the Balkans is too weak and displaced to the southwest. Thus, this result supports our argument that, in nature, this trough and its associated mid-level cooling are instrumental in favoring local convection over the Balkans/Italy. Because the large-scale surface impact of the SNAO is misrepresented in this model, so is the precipitation seesaw between northwestern Europe and the Mediterranean region, which is virtually absent in the model (cf. Fig. 14a with Fig. 7b).

The GFDL-CM2.1 model does a somewhat better job of reproducing the surface signature of the SNAO, as can be seen in the right panels of Figs. 13 and 14, which display corresponding results for run-1 of the 20C3M/SRESA1B simulation. Of the three available GFDL-CM2.1 simulations (which differ only in their initial conditions), this is the one that yields the best results in terms of both the spatial pattern of the SNAO and its impact on precipitation, and so it is presented here as a best case scenario. The SNAO appears slightly better reproduced than in the HadCM3 model ($r_s = 0.91$ vs. 0.86) and the pattern of

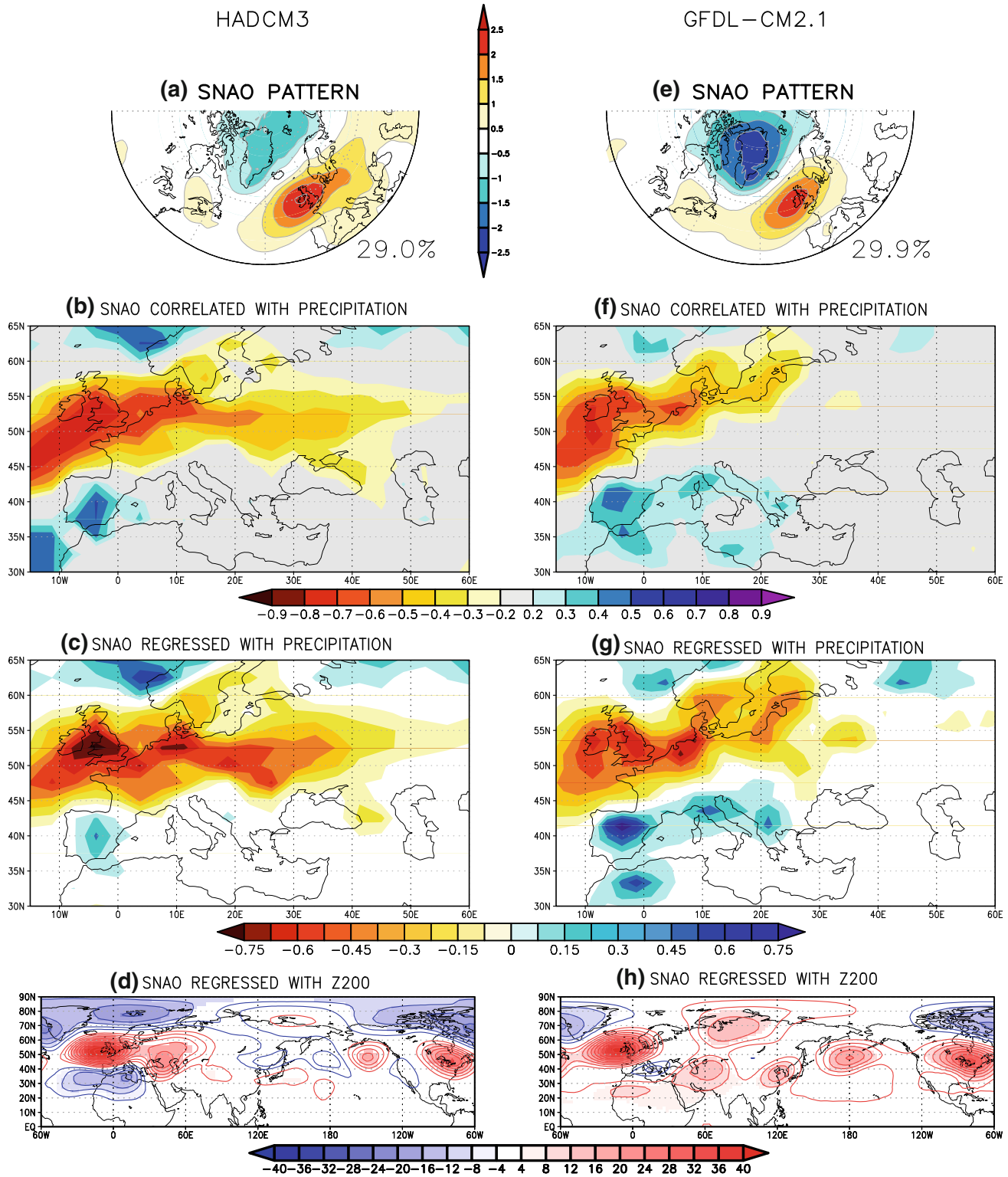

Fig. 13 *Left panels* The leading EOF of SLP in the HadCM3 simulation, computed for the 1950–2010 period and the SNAO domain (i.e., the model SNAO). The EOF is presented in terms of regressions between the detrended normalized time series of the EOF (SNAO index) and detrended SLP anomalies at every grid-point. Contour interval is 0.5 hPa/SD. *Middle panels*: Same but for correlation and regression of precipitation onto the SNAO index (contour interval is 0.1 and 0.075 mm/day, respectively). Correlations less than 0.2 (which do not pass a two-sided significance test at the 90% level) are not plotted. *Bottom panels*: same but for regressions of Z-200 hPa anomalies (contour interval is 4 m; regressions that pass a two-sided 95% significance test are also *shaded*). *Right panels*: Same for run 1 of the GFDL-CM2.1 model. Note that results are very similar when the trends are not removed, despite the strong trend in the SNAO in GFDL-CM2.1 (Fig. 15)

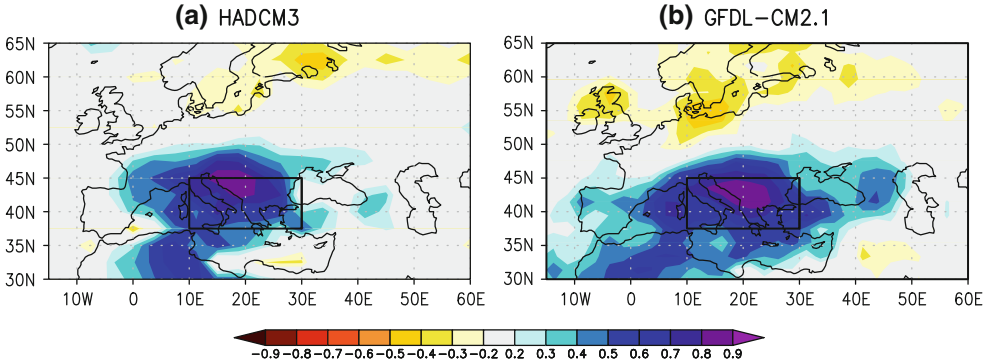

Fig. 14 Like Fig. 7b but for model data. Correlation between JA mean precipitation in the Balkan/Italy region (see box) and precipitation at every grid-point in the HadCM3 and GFDL-CM2.1 simulations (1950–2010 period)

positive precipitation correlations/regressions over the northern Mediterranean region, though still weaker than in observations, now extends to Italy and the Balkans (Fig. 13f, g). The associated Z-200 field now features a trough directly over the Balkans, albeit a very weak one (note that its significance is higher than the two-sided significance indicates, since the sign is now expected a priori). However, there is no trough over Iberia, where the precipitation anomalies are strongest, and overall the SNAO related wavetrain is not well replicated. Still, in the other two GFDL-CM2.1 simulations, in which the observed precipitation correlations in Italy and the Balkans are even more poorly reproduced, the 200-hPa trough is either absent or displaced south, which lends some credence to the hypothesis that mid-level cooling is important. Nevertheless, the strength of the simulated precipitation see-saw between the Balkans/Italy region and northern Europe is still underestimated (cf. Figs. 7b and 14b), even in this best case scenario.

The failure of these two GCMs to capture the observed pattern of increased precipitation in southern Europe during summers with a positive NAO is a matter of concern for simulations of future climate because these models predict a strong upward trend in the SNAO, as was already shown in F2009 for the HadCM3 transient simulation. To show that this trend is also present in the SRESA1B simulation for this model as well as in the GFDL model, we proceed as in F2009 and project each model's own SNAO "baseline" pattern (1950–2010 EOF-1) onto the full 1860–2100 SLP time series (unlike F2009, for simplicity, we project over the same domain in which the EOF is computed). For the HadCM3 model, also following F2009, we subtract the area-mean SLP north of 30°N in order to remove a uniform negative extratropical SLP trend signal. Figure 15 shows the evolution of the SNAO for the entire time series and for both models, together with trend lines computed for the 1860-2010 and the 2010-2100 periods. The future upward trend is particularly strong in the GFDL model (1.78 ± 0.58 SD/century—two standard errors), where it is already evident and very significant in the previous period (0.55 ± 0.30 SD/century[9]). In contrast, the past trend is weak and not significant in HadCM3 and only emerges clearly in the twenty-first century (1.44 ± 0.65 SD/century), which is more consistent with the behavior of the observed SNAO (Fig. 3; Table 1). Note that both models simulate realistic levels of multidecadal variability.

It now becomes evident that, given this strong future SNAO trend, the errors in representing the influence of the SNAO will impact the projected precipitation trends in the Mediterranean region. These trends, with and without the influence of the SNAO, are shown in Fig. 16 for the 2010–2100 period. The positive SNAO trend roughly accounts for 50% or more of the projected precipitation decrease north of 50°N in both models, particularly for the GFDL model where this proportion is close to 100% in the UK and Scandinavia (Fig. 16, middle panels). Over Iberia, where a positive SNAO leads to weak increases in precipitation (Fig. 13), this influence acts to slightly offset the drying due to other mechanisms. An even larger offset would also be evident over the northeastern Mediterranean if the impact of the SNAO were correctly simulated by these models. For instance, over the northern Balkans/Italy, where the magnitude of the observed SNAO/precipitation regression is greater than 0.3 mm/day (Fig. 6a, 10a), the projected SNAO trend would result in $\sim$0.05 mm/day/decade increases in precipitation, enough to almost cancel out the drying due to non-NAO related mechanisms. Note that the large upward SNAO trend accounts for the enhanced summer drying in Europe in these two models, compared to other models or the multi-model ensemble

[9] We have verified that this SNAO trend is not associated with climate drift in the GFDL-CM2.1 model: the SNAO trend in the first 300 years of the corresponding control run (Knutson et al. 2006), obtained once again by projecting the model's SNAO pattern, is one order of magnitude smaller and not statistically significant (regardless of which of the runs is used to define the pattern).

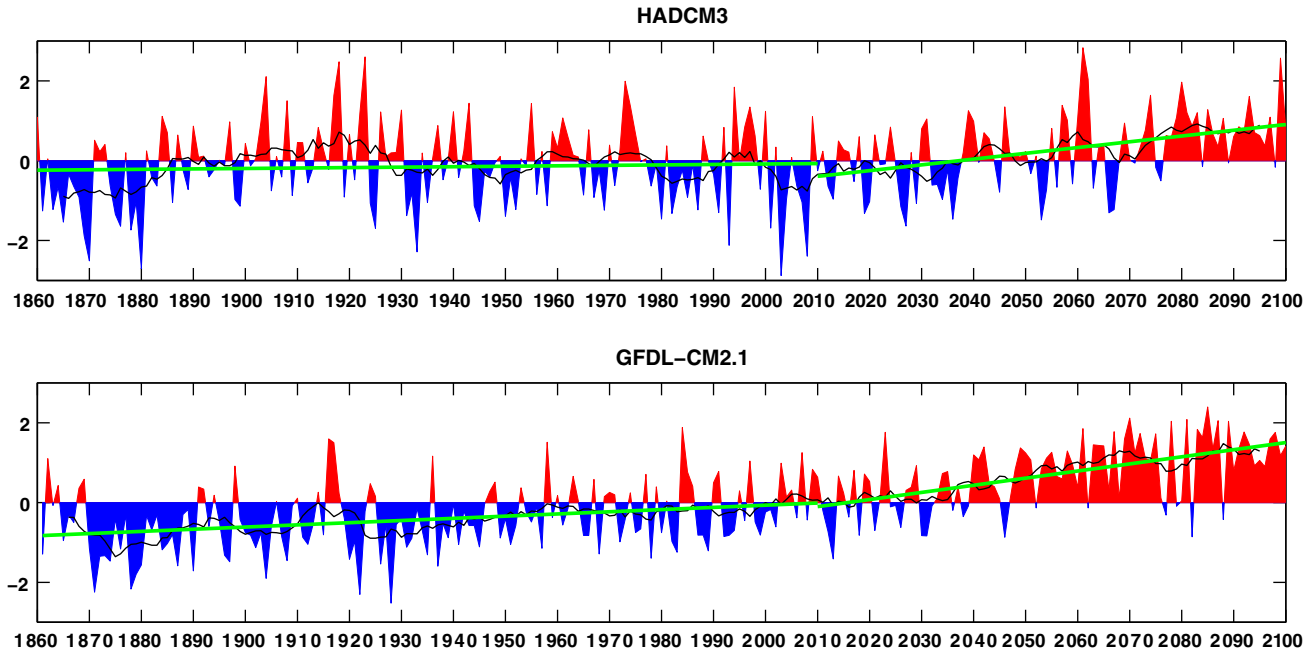

Fig. 15 Normalized time series of the SNAO (computed as a projection onto the 1950–2010 leading EOF) in the 20C3M-SRES1AB simulation in HadCM3 (*top*) and GFDL-CM2.1-run1 (*bottom*), from 1860 to 2100. The *black curve* depicts a 9-year running mean. The *green lines* indicate the linear trends from 1860 to 2010 and from 2010 to 2100

mean (Fig. 17). We conclude that these two models appear to be overestimating future precipitation decreases in the Mediterranean region, provided the projected increase in the SNAO is realized.

8 Conclusions

Though less robust and extensive than its winter counterpart, the SNAO is nonetheless a prominent feature of summer atmospheric variability in the North Atlantic/European sector, with a pattern of SLP anomalies that is characterized by a strong anticyclonic (cyclonic) circulation over the UK and northwest Europe (Greenland) during the positive phase. The SNAO directly and strongly influences the surface climate of northwest Europe, as previously documented (F2009), but it also significantly modulates temperature and precipitation in the northern Mediterranean region, particularly Spain, Italy and the Balkans. Because we were interested in examining the connection between the SNAO and projected drying in this region, we have focused on the SNAO impacts on precipitation.

We have found that not only is the signature of the SNAO in the Mediterranean linear and robust, typified by wetter than normal conditions during high SNAO summers (July–August), but it is consistent with a hemispheric upper-level circulation that (in this phase) includes a prominent trough centered over the Balkans, which leads to mid-tropospheric cooling and increased potential instability in the region. Because this enhanced precipitation is accompanied by dry conditions in the direct vicinity of the UK anticyclone, the influence of the SNAO is thus characterized by a strong north–south dipole in precipitation between northwest Europe and the Mediterranean.

We have also examined two CMIP3 models (HadCM3 and GFDL-CM2.1) to assess the degree of realism of the SNAO impact and the extent to which predicted future changes in precipitation in Europe are related to variations in the SNAO. In these two models, the spatial pattern of the SNAO is correctly reproduced and a strong upward SNAO trend is projected for the twenty-first century. This tendency towards persistent anticyclonic conditions over northwest Europe explains a good portion (between 40 and 100%) of the projected drying in this region, particularly in the GFDL model.

There are several problems with this result. The first relates to the magnitude of the projected SNAO trend, which appears to be quite model dependent. Indeed, these two models were chosen precisely because of their large SNAO trend. Other CMIP3 models exhibit a weaker trend or no trend at all (Bladé et al. in preparation), whereas the trend in the GFDL model is so strong that it is already present and significant in the twentieth century. Furthermore, the plausibility of this trend cannot be assessed on the basis of current observations. Although the SNAO appeared to exhibit a strong preference for the positive phase between 1967 and 2000, the full historical record

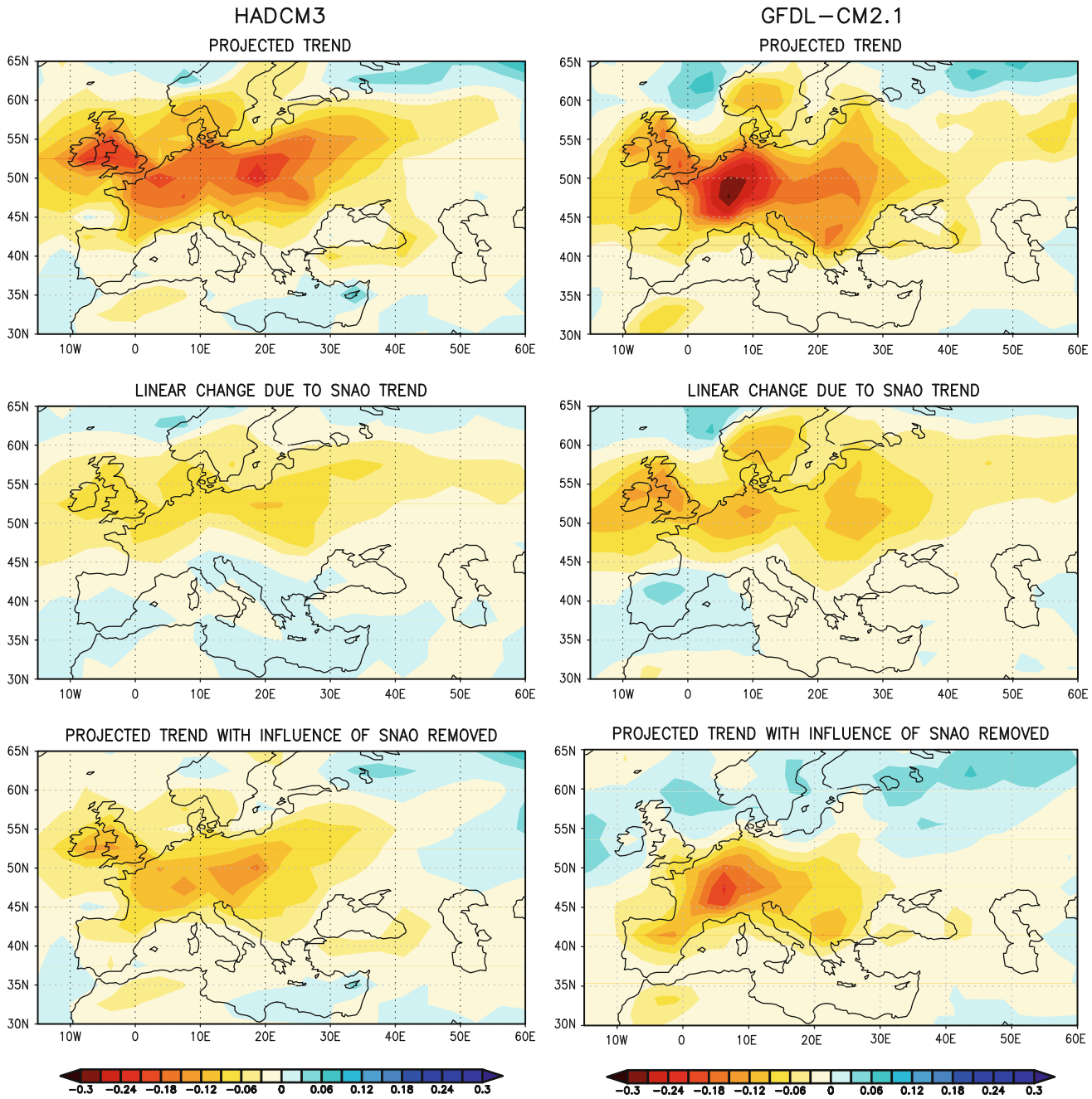

Fig. 16 *Left panels*: Future 2010–2100 linear trend in summer precipitation in the HadCM3 simulation (*top*), linear trend due to the SNAO influence (*middle*) and trend with the influence of the SNAO removed (*bottom*). Units are mm/day/decade. *Right panels*: Same but for the GFDL-CM2.1-run 1 simulation

(including the recent years) does not provide unequivocal evidence of a persistent and statistically significant upward trend that would lend credence to the projected model trend (although the observations do not disprove it either). Since much of the anticipated drying in northwestern Europe in the two models examined is related to this predicted upward SNAO trend, the intensity of this drying becomes uncertain. The projected precipitation decrease in these two models is particularly pronounced, compared to the other CMIP3 models, precisely because of this strong SNAO trend.

The second concern is that, based on the observed relation between the SNAO and precipitation, we would expect the upward SNAO trend to be accompanied by an increase in precipitation in parts of the Mediterranean, which would partially compensate the drying due to other processes, such as soil moisture feedbacks and increased land-sea temperature contrasts. However, the models fail to

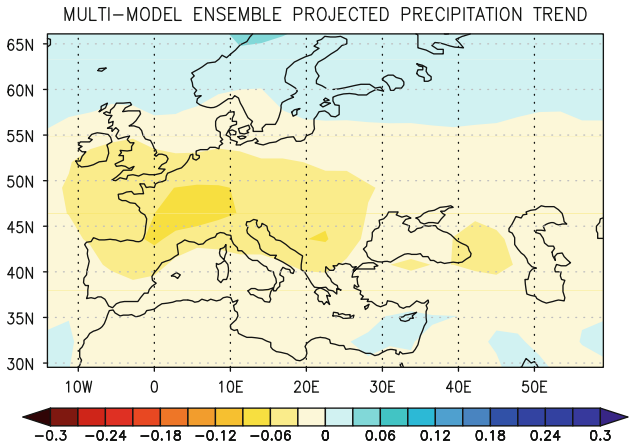

Fig. 17 2010–2100 summer (JA) precipitation trend in the CMIP3 multi-model ensemble mean. Units are mm/day/decade. The 23 models for which data is available in the PCMDI archive were linearly interpolated to a common 2.5° grid. For each model all available ensemble members have been averaged and then the multi-model mean has been computed, so that all 23 models are weighted equally

capture the impact of the SNAO in this region, with a weak or virtually no response in the eastern Mediterranean region, and so this compensation does not occur. The models' misrepresentation of the influence of the SNAO appears to be related to errors in the simulation of the upper-level circulation that develops downstream of the SNAO dipole location, which in turn may be due to deficiencies in the depiction of the summer jet. Future research will examine the behavior of the SNAO in other climate models, address the causes for the errors in the simulated SNAO teleconnections and investigate the dynamical mechanisms responsible for the upward SNAO trend. Another potential issue of interest is the robustness and stationarity of the SNAO pattern in models.

Our results agree with Boé et al. (2009) who used an analog method applied to daily data and a subset of 15 CMIP3 models. They concluded that large-scale circulation changes do not drive future summer precipitation decreases in the Mediterranean region but that increased occurrence of the positive SNAO regime contributes to the reduction in precipitation in northwest Europe, with a large inter-model spread in the changes in SNAO+ frequency leading to a large spread in the magnitude of the drying (these results are also qualitatively consistent with Rowell and Jones 2006). Our analysis, however, suggests that the first finding—no role for large-scale dynamics in the drying of the Mediterranean region—should be viewed as resulting from model errors since the observed linkage between the SNAO and precipitation in the Mediterranean is absent in the models. Another impact of the SNAO that may be missed by the models is a potential reduction of drying in *central* Europe. If the SNAO becomes increasingly positive in the future, the increased precipitation (or offset drying) in the eastern Mediterranean may act to weaken the heat low that tends to develop in response to surface warming and soil-moisture depletion (Haarsma et al. 2009). Since this heat low brings enhanced dry easterly winds into central Europe, drying in this region would also be diminished.

A final caveat concerning the strong future precipitation decreases anticipated by some CMIP3 models is that, for now, observed summer precipitation in Europe does not exhibit statistically significant negative trends, neither short-term (1950–2010) nor long-term (1900–2010), except in parts of the UK. This result holds true in all datasets examined and stands contrary to some studies that conclude that summer precipitation in the Mediterranean region has decreased, based on the comparison of mean precipitation between two arbitrary multi-decadal periods (Pal et al. 2004; Giorgi and Lionello 2008).

In conclusion, our analysis suggests that projections of summer precipitation reduction in Europe/Mediterranean are highly uncertain. In particular, if the upward SNAO trend is verified, drying over the Mediterranean region could be less drastic than the models anticipate.

Acknowledgments We thank Pablo Zurita for his comments on the manuscript and Nate Mantua, Javier García-Serrano and Vicent Altava for useful discussion of our work. We also thank Ricardo Trigo and an anonymous reviewer for their useful suggestions, which have helped clarify several points in the manuscript. Roy Mendelssohn kindly supplied the SST data. DF was supported by grant Consolider 2007-CSD2007-00050. The work was funded by grant CGL2009-06944 of the Spanish MICINN. We acknowledge the modeling groups, the Program for Climate Model Diagnosis and Intercomparison (PCMDI) and the WCRP's Working Group on Coupled Modelling (WGCM) for their roles in making available the WCRP CMIP3 multi-model dataset. Support of this dataset is provided by the Office of Science, U.S. Department of Energy.

References

Ansell TJ et al (2006) Daily mean sea level pressure reconstructions for the European-North Atlantic region for the period 1850–2003. J Climate 19:2717–2742

Barnston AG, Livezey RE (1987) Classification, seasonality and persistence of low-frequency atmospheric circulation patterns. Mon Wea Rev 115:1083–1126

Boé J, Terray L, Cassou C, Najac J (2009) Uncertainties in European summer precipitation changes: role of large scale circulation. Clim Dyn 33:265–276

Branstator G (2002) Circumglobal teleconnections, the jet stream waveguide, and the North Atlantic Oscillation. J Climate 15:1893–1910

Chronis T, Raitsos DE, Kassis D, Sarantopoulos A (2011) The summer North Atlantic Oscillation Influence on the Eastern Mediterranean. J Climate 24:5584–5596. doi:10.1175/2011JCLI3839.1

Feidas H, Noulopoulou N, Makrogiannis T, Bora-Senta E (2007) Trend analysis of precipitation time series in Greece and their

relationship with circulation using surface and satellite data: 1955–2001. Theor Appl Climatol 87:155–177
Feldstein SB (2007) The dynamics of the North Atlantic Oscillation during the summer season. Quart J Roy Meteor Soc 133:1509–1518
Folland CK, Knight J, Linderholm HW, Fereday D, Ineson S, Hurrell JW (2009) The summer North Atlantic Oscillation: past, present, and future. J Climate 22:1082–1103
Giorgi F, Lionello P (2008) Climate change projections for the Mediterranean region. Global Planet Change 63:90–104
Greatbatch RJ, Rong P–P (2006) Discrepancies between different Northern Hemisphere summer atmospheric data products. J Climate 19:1261–1273
Haarsma RJ, Selten F, vd Hurk B, Hazeleger W, Wang X (2009) Drier Mediterranean soils due to greenhouse warming bring easterly winds over summertime central Europe. Geophys Res Lett 36:L04705. doi:10.1029/2008GL036617
Hatzianastassiou N, Katsoulis B, Pnevmatikos J, Antakis V (2008) Spatial and temporal variation of precipitation in Greece and surrounding regions based on global precipitation climatology project data. J Climate 21:1349–1370
Haylock MR, Hofstra N, Klein Tank AMG, Klok EJ, Jones PD, New M (2008) A European daily high-resolution gridded data set of surface temperature and precipitation for 1950–2006. J Geophys Res 113:D20119
Hulme M, Osborn TJ, Johns TC (1998) Precipitation sensitivity to global warming: comparison of observations with HadCM2 simulations. Geophys Res Lett 25:3379–3382
Hurrell JW (1995) Decadal trends in the North Atlantic Oscillation: regional temperatures and precipitation. Science 269:676–679
Hurrell JW, Deser C (2009) North Atlantic climate variability: the role of the North Atlantic Oscillation. J Mar Syst 78(1):28–41. doi:10.1016/j.jmarsys.2008.11.026
Hurrell JW, Folland CK (2002). A change in the summer circulation over the North Atlantic. *CLIVAR Exchanges,* No. 25, International CLIVAR Project Office, Southampton, United Kingdom, pp 52–54
Hurrell JW, Kushnir Y, Ottersen G, Visbeck M (2003) An overview of the North Atlantic Oscillation. The North Atlantic Oscillation: climatic significance and environmental impact. Geophys Monogr. Am Geophys Union 134:1–35
Jones PD, Jonsson T, Wheeler D (1997) Extension to the North Atlantic Oscillation using early instrumental pressure observations from Gibraltar and South-West Iceland. Int J Climatol 17:1433–1450
Kalnay E et al. (1996) The NCEP/NCAR 40-year reanalysis project. Bull Am Meteor Soc 77:437–471
Knutson TR, Delworth TL, Dixon KW, Held IM, Lu J, Ramaswamy V, Schwarzkopf MD, Stenchikov G, Stouffer RJ (2006) Assessment of twentieth-century regional surface temperature trends using the GFDL CM2 coupled models. J Climate 19:1624–1651
Liebmann B, Dole RM, Jones C, Bladé I, Allured D (2010) Influence of choice of time period on global surface temperature trend estimates. Bull Am Meteorol Soc 91:1485–1491
Mariotti A, Arkin P (2007) The North Atlantic Oscillation and oceanic precipitation variability. Clim Dyn 28(1):35–51
Mariotti A, Dell'Aquila A (2011) Decadal climate variability in the mediterranean region: roles of large-scale forcings and regional processes. Clim Dyn (in press). doi:10.1007/s00382-011-1056-7
Meehl GA et al. (2007) Global climate projections. In: Solomon S et al. (eds) Climate change 2007: the physical science basis. Cambridge University Press, Cambridge, pp 747–845
Mitchell TD, Jones PD (2005) An improved method of constructing a database of monthly climate observations and associated high-resolution grids. Int J Clim 25:693–712
North GR, Bell TL, Cahalan RF, Moeng FJ (1982) Sampling errors in the estimation of empirical orthogonal functions. Mon Wea Rev 110:699–706
Obregón A, Bissolli P, Kennedy JJ, Parker DE (2010) Regional climates: Europe [in "State of the Climate in 2009"]. Bull Am Meteor Soc 91(7):S160–S162
Pal JS, Giorgi F, Bi X (2004) Consistency of recent European summer precipitation trends and extremes with future regional climate projections. Geophys Res Lett 31:L13202. doi:10.1029/2004GL019836
Portis DH, Walsh JE, El Hamly M, Lamb PJ (2001) Seasonality of the North Atlantic Oscillation. J Clim 14:2069–2078
Reynolds RW, Smith TM, Liu C, Chelton DB, Casey KS, Schlax MG (2007) Daily high-resolution-blended analyses for sea surface temperature. J Clim 20:5473–5496
Rodwell MJ, Hoskins BJ (1996) Monsoons and the dynamics of deserts. Quart J Roy Meteor Soc 122:1385–1404
Rowell DP, Jones RG (2006) Causes and uncertainty of future summer drying over Europe. Clim Dyn 27:281–299. doi:10.1007/s00382-006-0125-9
Rudolf B, Schneider U (2005) Calculation of gridded precipitation data for the global land-surface using in situ gauge observations. In: Proceedings of the 2nd workshop of the International Precipitation Working Group IPWG. Monterey, 2004, pp 231–247
Sun J, Huijun W, Wei Y (2009) Role of the tropical Atlantic sea surface temperature in the decadal change of the summer North Atlantic Oscillation. J Geophys Res 114:D20110. doi:10.1029/2009JD01239
Trenberth KE, Paolino DA Jr (1980) The Northern Hemisphere sea-level pressure data set: trends, errors and discontinuities. Mon Wea Rev 108:855–872
Watanabe M (2004) Asian jet waveguide and a downstream extension of the North Atlantic Oscillation. J Clim 17:4674–4691
Zveryaev II, Allan RP (2010) Summertime precipitation variability over Europe and links to atmospheric dynamics and precipitation. J Geophys Res 115:D12102. doi:10.1029/2008JD011213